

## Biomedical Paper

# Computer Model for Cryosurgery of the Prostate

Monika Jankun, B.S., T. J. Kelly, B.S., Amjad Zaim, M.S., Karen Young, M.S., Rick W. Keck, B.S., Steven H. Selman, M.D., and Jerzy Jankun, Ph.D.

*Urology Research Center, Department of Urology (M.J., T.J.K., A.Z., K.Y., R.W.K., S.H.S., J.J.), and Department of Physiology and Molecular Medicine (S.H.S., J.J.), Medical College of Ohio, and Department of Bioengineering, University of Toledo (A.Z., K.Y., S.H.S., J.J.), Toledo, Ohio*

**ABSTRACT** The objective of this study was to devise an interactive tool to assist in cryoablation therapy through computer modeling, simulation, and visualization. CryoSim, a software package, accepts a set of acquired and processed three-dimensional ultrasound images, then models heat diffusion (formation of the iceball) based on numerical approximation of the heat equation and knowledge of the thermal properties of the underlying tissues. Results of cryoexperiments were found to be significantly similar to those generated by CryoSim. Therefore, CryoSim provides a viable technique for predicting the outcome of cryosurgery, and establishes a platform for future automation of cryosurgery. *Comp Aid Surg* 4:193-199 (1999). ©1999 Wiley-Liss, Inc.

**Key words:** cryosurgery, prostate cancer, three-dimensional ultrasound, computer modeling

## OBJECTIVE

Prostate cancer is the second leading cause of cancer death in American men. In 1997, approximately 209,900 new cases of prostate cancer were diagnosed, and the disease resulted in more than 41,800 deaths.<sup>7,18</sup> Traditional treatments for prostate cancer include surgical removal or radiation therapy. Recently, however, cryosurgery has been accepted as a treatment option in localized carcinoma of the prostate, in part because of new technological advances and a refinement of the technique by Onik et al.<sup>9,19</sup> Prostate cryosurgery has certain advantages over other procedures, including lower morbidity, short hospital stay, minimal blood loss, and the ability to retreat patients when necessary.<sup>1,5,8</sup>

Cryoablation therapy is a method of minimally invasive cancer treatment that uses liquid nitrogen or supercooled argon to freeze and thus destroy tumors. Liquid nitrogen cools the tumor via a set of cryoprobes which have adjustable flow

rates, cooling temperatures, and activation times. Although cryoablation has been used for some time, the efficacy of the cryoprobe system has not been extensively studied. Cryosurgery of the prostate is performed under ultrasound monitoring. Unfortunately, the iceball of frozen tissue obstructs the propagation of sound waves, and only the front of this ball is visible. In addition, whereas the temperature of the leading front of the iceball in the prostate is  $-8^{\circ}\text{C}$ , the temperature needed to kill the tissue has been reported to be between  $-40^{\circ}$  and  $-50^{\circ}\text{C}$ .<sup>16</sup> At present, it is difficult to monitor the temperature of the prostate as it is being frozen. Two- and three-dimensional (2D and 3D) modeling of cryosurgery has been described in numerous papers, but there have been no studies of cryosimulation of the prostate in 3D models.<sup>2,11,13-15</sup> We have therefore developed a computer program to model cryosurgery mathematically. This tool mon-

Received November 24, 1998; accepted July 19, 1999.

Address correspondence/reprint requests to: Dr. Jerzy Jankun, Urology Research Center, Department of Urology, Medical College of Ohio, 3000 Arlington Avenue, Toledo, OH 43699-0008. E-mail:jerzy@golemxiv.dh.mco.edu.

©1999 Wiley-Liss, Inc.

itors the boundary of destroyed tissue and neighboring organs in 3D based on ultrasound images. The Cryoablation Simulator (or CryoSim) provides a modeling, training, and automation platform for cryoablation therapy. Provided with the physical characteristics of the surrounding tissue, a 3D ultrasound of the affected region, and the positions and settings of the cryoprobes, CryoSim calculates the isotherms of the frozen tissues or killing region. These isotherms are depicted visually with reference to the surrounding tissue. Within the simulator, the user may move the cryoprobes, change their settings, and adjust the viewpoint. CryoSim was developed using C++ and Direct3D, a graphical library for Windows 95 and Windows NT. Although the initial effort concentrated on the applications of this program in cryosurgery of the prostate, the program could also be used in cryoablation of different organs if their thermal properties are known.

## MATERIALS AND METHODS

### 3D Model of the Prostate

The ultrasound data were obtained using an Aloka 7.5-MHz linear array transducer and 5-MHz curved array sector transducer (UST-664-5/7.5; Aloka Co, Wallingford, CT) and a prostate phantom (Model 84-353; Nuclear Associates, Carle Place, NY) or chicken breast. This was followed by reconstruction of 3D models as described below. The ultrasound data, composed of successive 8-bit unsigned integers, specifies the intensity of the imaged voxel. No header is provided, so the user must specify the voxel size. In addition, the width, height, and depth of the ultrasound picture must also be specified by providing dimensions for the individual voxel (in inches or centimeters). The picture size determines the size of the file: The voxel size scales the data file to the image dimensions (inches or centimeters). The size of the scanned ultrasound object was verified by producing images of objects with known spatial dimensions and comparing them with their scale on the computer screen. The first 2D image of the object sets up the angular orientation of the object, e.g., the zero coordinate on the  $z$  axis in Cartesian coordinates, with each succeeding layer being on top of the previous one, whereas the thickness of each layer is defined by the  $z$  dimension of each voxel.

### Image Acquisition

In the first step, 3D transrectal ultrasound data of the prostate are acquired by rotating the ultrasound probe in the lateral direction by fixed angle incre-

ments. As the probe rotates, a frame-grabber converts the stream of data produced by the ultrasound machine into a digital image which is stored on a disk for later analysis.

### Fan-to-Rectangular Conversion

As the ultrasound probe sweeps across the prostatic volume, a fan-shaped swept volume is produced. In this configuration, the acquired images are arranged as a fan of (typically) 100 2D images, radiating outward from the ultrasound transducer, and evenly spaced over an arc of (typically)  $80^\circ$ . The reconstruction algorithm of the existing 3D visualization software produces a 3D image in which the relative orientation of the acquired images is uniformly preserved. Conversion of the data from a fan-shape geometry to a uniform rectangular-grid geometry using polar-to-Cartesian coordinate mapping is needed for proper 3D reconstruction. We use bilinear interpolation as a conversion algorithm to convert a set of 2D images to 3D.<sup>3,4,17</sup>

### Theoretical Basis of Cryoablation Modeling

The CryoSim program uses a partial differential equation (PDE) to describe the growth of the freezing front in the tissue. The PDE used is the classic heat equation<sup>12</sup>:

$$\nabla(k\nabla T) = c\rho \frac{\partial T}{\partial t} - \dot{q} \quad (1)$$

where  $T$  represents the temperature and is a function of space and time (in three dimensions,  $x$ ,  $y$ , and  $z$ ),  $k$  is the thermal conductivity of the substance (W/m K),  $c$  is the specific heat (J/kg K),  $\rho$  is the density (kg/m<sup>3</sup>), and  $\dot{q}$  is the heat flux per unit volume (J/s). In our derivation, we will assume that  $k$  and  $\dot{q}$  are constant in the separate regions of interest, i.e., the frozen and solid areas of a tissue, and averaged for the "slush" intermediate region, so the spatial derivatives only apply to the temperature.

The solution to this PDE involves numerical approximation to the derivatives and knowledge of the boundary conditions. In our case, we have boundaries at the cryoprobes and an initial temperature distribution. We used a backward difference method since it is unconditionally stable when compared to Robin's forward method.<sup>12</sup>

This parabolic PDE is analyzed in two parts: the spatial (double) derivative and the derivative in time. All numerical approximations to derivatives are based on Taylor approximations: The method (forward, central, or backward) describes whether

the delta in the approximated dimension is positive, negative, or, in the case of central, averaged between the two. A central technique is used for the second derivative, whereas a backward difference method is used for the single derivative. For a spatial derivative, the approximation is:

$$\frac{\partial^2 T}{\partial x^2} = \frac{T(x - \Delta x) - 2T(x) + T(x + \Delta x)}{\Delta x^2} \quad (2)$$

For the time derivative, the approximation is:

$$\frac{\partial T}{\partial t} = \frac{T(t) - T(t - \Delta t)}{\Delta t} \quad (3)$$

With these two approximations, we can derive the approximation formula used in our algorithm. First, we start with the original PDE

$$k \nabla^2 T = c \rho \frac{\partial T}{\partial t} - \dot{q} \quad (4)$$

Now, we apply the approximations to obtain

$$\begin{aligned} k \left( \frac{T(x - h) - 2T(x) + T(x + h)}{h^2} \right. \\ + \frac{T(y - h) - 2T(y) + T(y + h)}{h^2} \\ \left. + \frac{T(z - h) - 2T(z) + T(z + h)}{h^2} \right) \\ = c \rho \frac{T(t) - T(t - \Delta t)}{\Delta t} - \dot{q} \end{aligned}$$

or, more simply,

$$k \sum_j \frac{T_{j,t} - T_{i,t}}{h^2} = c \rho \frac{T_{i,t} - T_{i,t-1}}{\Delta t} - \dot{q}_{i,t} \quad (5)$$

where  $h$  is the spatial step size of the grid (uniform in all directions),  $i$  indexes the temperature value at the current mesh point of interest,  $j$  indexes the temperature value at  $i$ 's six nearest neighbors, and  $t$  and  $t-1$  are the current and previous time steps, respectively. Also, to perform this approximation, the continuous 3D space must be broken into several finite elements that share the average of all the thermal properties in that element. Thus, the finer the spacing is, the more information is retained. However, smaller spacing also dramatically in-

**Table 1. Thermal Properties of Poultry and Prostate<sup>10</sup>**

Material	$\rho$ (kg/m <sup>3</sup> )	$K$ (W/m K)	$c_p$ (J/kg K)	$\Delta H^{SL}$ (J/kg)
Chicken				
Unfrozen	1050	0.50	3310	246,556
Frozen	910	1.68	1550	
Prostate				
Unfrozen	1086	0.45	3520	268,000
Frozen	1034	2.0	1840	
Beef (25°C)	2174	0.47	2956	206,819
Banana				
Unfrozen	2801		3347	309,184
Frozen	1470		1757	

creases the memory and time needed for computation.

In this approximation, we are interested in knowing the temperature at all points at a specific time  $t$ . Thus, we solve for this time step in our approximation. We could rewrite Equation (3) by solving for  $T_{i,t}$ , but it is more convenient to put it in a form that can be solved using matrix manipulation, such as

$$A \mathbf{T}_t = \mathbf{T}_{t-1} + \mathbf{K} \quad (6)$$

where  $A$  is our coefficient matrix, the  $\mathbf{T}$  vectors represent the current and previous temperature values, respectively, and the  $\mathbf{K}$  vector is a constant vector encapsulating heat sources and sinks. This matrix is determined by the following equation:

$$T_{i,t} - \frac{\Delta t}{c \rho} k \sum_j \frac{T_{j,t} - T_{i,t}}{h^2} = T_{i,t-1} + \frac{\Delta t}{c \rho} q \quad (7)$$

The preferred form of this equation is

$$(1 + 6\lambda) T_{i,t} - \lambda \sum_j T_{j,t} = T_{i,t-1} + \lambda \frac{h^2}{k} q_{i,t} \quad (8)$$

which has  $T_{i,t}$  isolated by itself and  $\lambda$  representing

$$\frac{\Delta t}{c \rho} \frac{k}{h^2}$$

This will produce a sparse matrix that is diagonally dominant.

### Computer Model of Cryosurgery

All computer simulations were done using the thermal properties shown in Table 1. Also, calculations were performed on the assumption that thermal

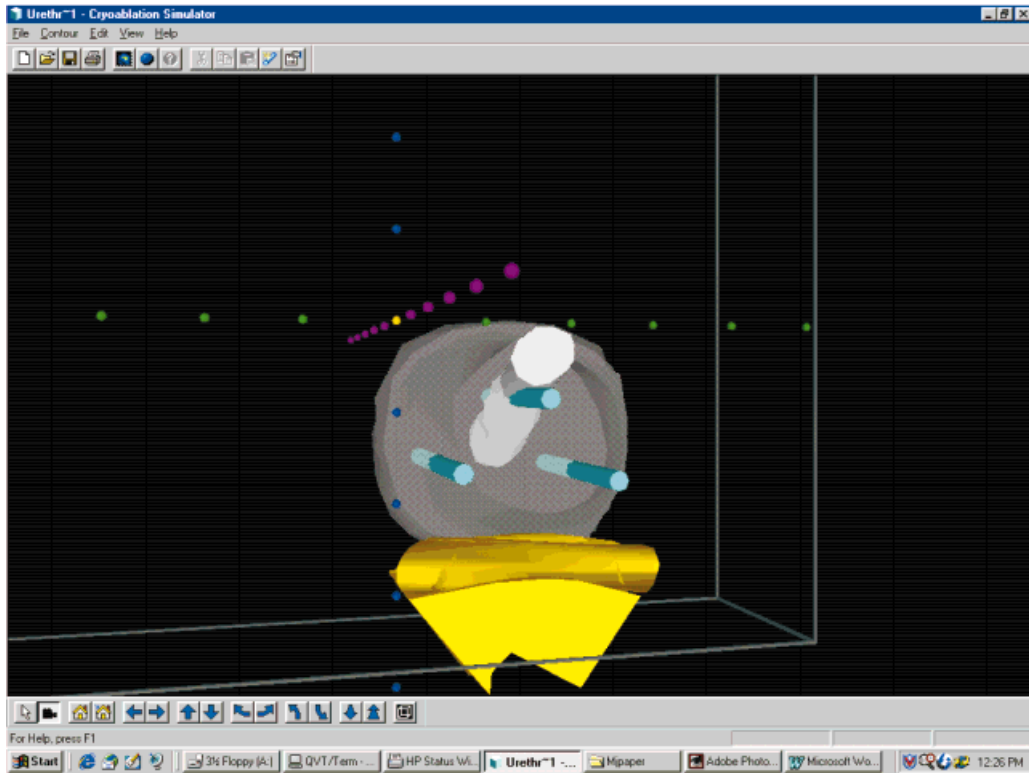


**Fig. 1.** Three-dimensional model of prostate phantom (light white), urethra (white), colon wall (yellow), and three cryoprobes (light blue).

properties are uniform throughout the prostate or any simulated organ. This is an obvious compromise between the time needed to do the calcula-

tions and a degree of imprecision that could eventually be introduced into this model.

A time step of 0.7 min and spatial step of 0.6

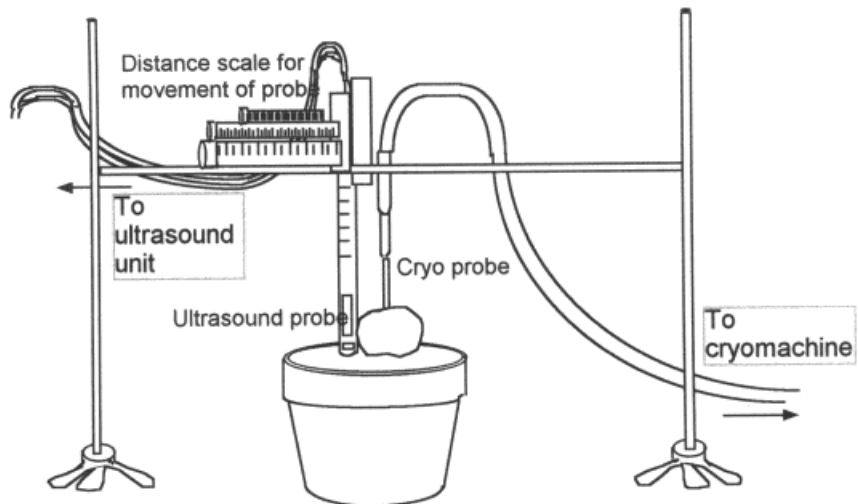


**Fig. 2.** Setup of cryoapparatus. The apparatus consists of the cryoprobe with the test object inserted on the tip, aligned to one side. The ultrasound probe and cryoprobe with test object were submerged in water. The adjustable scale was used to move the cryoprobe longitudinally to produce contiguous slices of the test object.

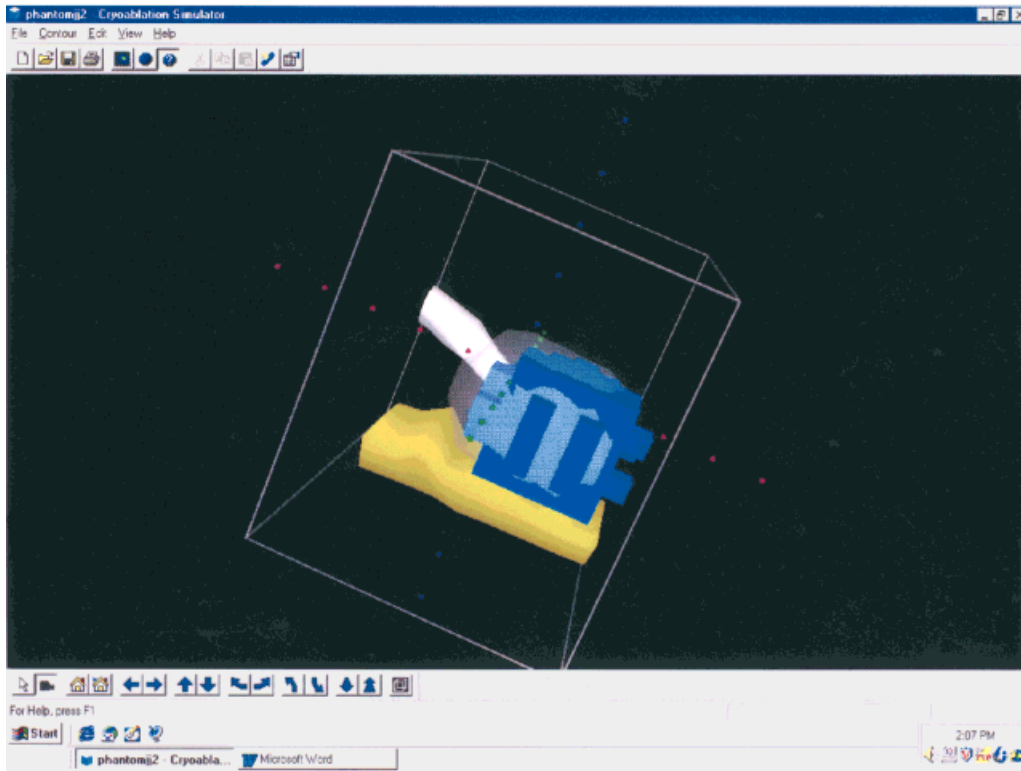


**Fig. 3.** A 3D plot of a prostate phantom produced by CryoSim showing the propagation of the freezing front or the iceball (blue) around the prostate volume after the insertion of two cryoprobes. Notice how the prostate is not fully enclosed by the iceball boundaries; simulation parameters should be adjusted accordingly.

cm were used. For cryoexperiment validation, we used one cryoprobe and stopped the calculation every 2 min from 4 to 16 min to measure the progress of iceball formation in the computer

model. Progress of iceball formation was measured from ultrasound images and was also calculated at 5-, 10-, and 15-min intervals for three cryoprobes. In addition, for visualization of iceball formation,

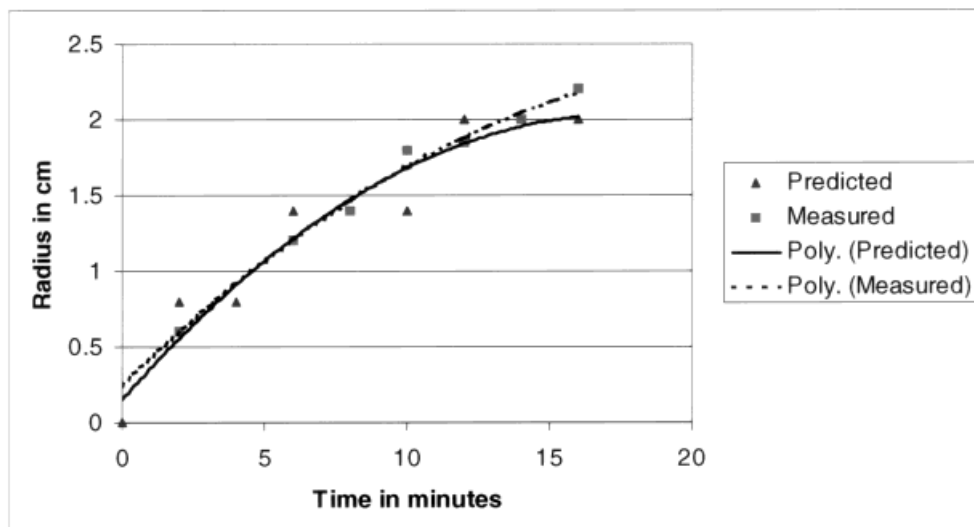


**Fig. 4.** Comparison of nonlinear regression of the measured radii (freezing distance) and computer-predicted leading front of the iceball. The solid line represents the best fit of measured distance; the dotted line represents the best fit of predicted distances.

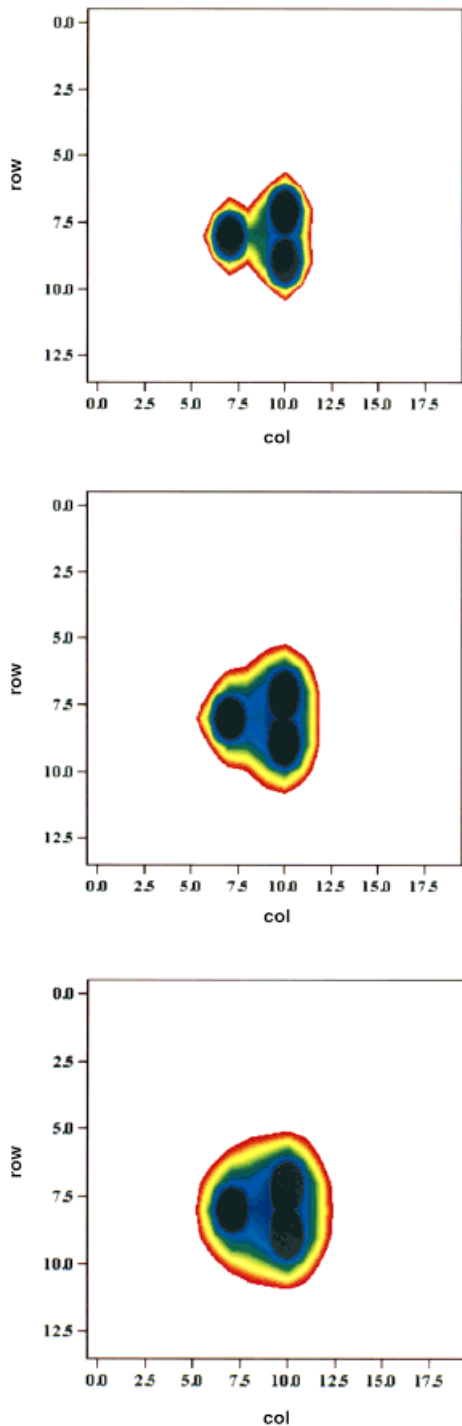


**Fig. 5.** Isotherms of frozen prostate. For simplicity, only isotherms between  $-8^{\circ}$  and  $-60^{\circ}\text{C}$  are shown. The white area represents temperatures between  $37^{\circ}$  and  $-8^{\circ}\text{C}$ ; black represents temperatures between  $-8^{\circ}$  and  $-180^{\circ}\text{C}$ .

we collected data on temperature distribution. For this, a time step of 0.8 min and spatial step of 0.7 cm were used. The isotherms were visualized by

the 3T3 Transform data visualization program (Fortner Sterling, VA), using the Interpolated Image function and Rainbow color table.

### Cryoexperiment

To validate predictions of the computer model with cryosurgery, we performed the cryo-experiment. In this experiment, the apparatus shown in Figure 2 was used. The basic setup consists of adjustable knobs that can move the ultrasound probe in a longitudinal and latitudinal direction. By moving the ultrasound probe in the longitudinal direction, we receive slice images of the object. The object was suspended using the cryoprobe inserted into it, then mounted securely to the apparatus. The suspended test object and cryoprobe were set in water beside the ultrasound probe. We used an Aloka 7.5-MHz linear array transducer and 5-MHz curved-array sector transducer (UST-664-5/7.5; Aloka). Chicken breasts were used because their thermal properties are very similar to those of the prostate gland (Table 1). The initial temperature of the water bath was  $12^{\circ}\text{C}$ .

Freezing was initiated by  $3 \times 4 \times 18\text{-mm}$  blunt cryoprobes (Accuprobe<sup>®</sup> 450; Cryomedical Sciences, Rockville, MD), using liquid nitrogen as a freezing medium. After freezing was initiated, images of the test object were taken at regular time intervals.

### RESULTS AND DISCUSSION

The 2D ultrasound images of chicken breasts were collected, 3D models were reconstructed by manual segmentation, and the cryoprobes were reproduced and positioned at relative coordinates corresponding to those of the real cryoprobes as shown in Figure 1. The cryoexperiment was initiated and data were collected as described in Materials and Methods. The size of the formed iceball was compared with that produced by CryoSym. Flow parameters and dimensions of the probe were at the same settings as on the cryomachine. Figure 3 shows a 3D plot of a prostate phantom with the iceball surface generated by CryoSim with one cryoprobe inserted. Figure 4 shows the nonlinear regression lines depicting cryoexperiment data and computer-generated radii of the iceball in the middle section of the prostate. The results show significant similarities between the data generated by CryoSim and the measurements of the iceball ( $p < .05$ ). The second-degree polynomial best fitting trend lines of measurements and model prediction are practically the same.

CryoSim provides for the possibility of modeling not only iceball formation, but also the tem-

perature distribution in 3D with up to eight cryoprobes. Our simulation used three cryoprobes and took readings at three time intervals (5, 10, and 15 min). The model revealed that the time needed to freeze the prostate is 10 min. This will be the time required if cryosurgery is monitored according to the expansion of the iceball under ultrasound. However, analysis of temperature distribution shows that the temperature gradient is very steep in the initial stages of cryosurgery, when  $-40^{\circ}$  to  $-50^{\circ}\text{C}$  isotherms are in proximity to the front of the iceball. As the freezing time progresses, the iceball becomes larger and the temperature gradient becomes much less steep (Fig. 5). The isotherm that has been reported to be therapeutic delimitates only approximately 50% of the iceball. Comparison of temperature isotherms shows that it is much more desirable to use multiple cryoprobes, e.g., five or more, for a short period of time. In such a configuration, the therapeutic isotherm is in proximity to the formed iceball front, thereby securing destruction of the gland.

The need for temperature monitoring and modeling of cryosurgery has been frequently emphasized, but studies have met with only limited success so far. CryoSim provides a new way to model the cryosurgery, display the leading front of frozen tissue in 3D, and display temperature distribution within the prostate. In this way, the simulator would present all data, such as the flow rate of each cryoprobe, its position, and the number of probes and cooling time needed for successful cryosurgery. CryoSim will also provide a platform for future automation of cryosurgery using a robotic arm to position the cryoprobes in a place that is predetermined as optimal by a computer program.

#### ACKNOWLEDGMENTS

This work was supported in part by grants from the Ohio Aerospace Institute/NASA, the OBR Research Challenge Fund, and the Stranahan Fund for Laser Research.

#### REFERENCES

1. Bischof JC, Merry N, Hulbert J. Design and characterization of an insulating probe. *Cryobiology* 1997; 34:80–92.
2. Budman HM, Dayan J, Shitzer A. Controlled freezing of nonideal solutions with application to cryosurgical processes. *J Biomech Eng* 1991;113:430–437.
3. Burden R, Faires J. Numerical analysis. 4th edition. Boston: PWS-KENT, 1989. 598 p.
4. Castleman KR. Digital image processing. Englewood, NJ: Prentice Hall, 1979. 429 p.
5. Connolly JA, Shinohara K, Presti JC, Carroll RP. Should cryosurgery be considered a therapeutic option in localized prostate cancer? *Urol Clin North Am* 1996;23:623–631.
6. Keanini RG, Rubinsky B. Optimization of multiprobe cryosurgery. *Trans ASME* 1992;114:796–802.
7. Naitoh J, Zeiner RL, Dekernion JB. Diagnosis and treatment of prostate cancer. *Am Fam Phys* 1998;57: 1531–1539.
8. Onik GM, Cohen JK, Reyes GD. Transrectal ultrasound-guided percutaneous radical cryosurgery ablation of the prostate. *Ca Cancer J Clin* 1993;72:1291.
9. Onik GM, Rubinsky B, Watson G, Ablin RJ. Percutaneous prostate cryoablation. St. Louis, MO: Quality Medical, 1995.
10. Peleg M. Physical properties of food. West Port, CT: AVI, 1983.
11. Poledna J, Berger W. A mathematical model of temperature distribution in frozen tissue. *Gen Physiol Biophys* 1986;15:3–15.
12. Rabin Y, Korin E. An efficient numerical solution for the multidimensional solidification (or melting) problem. *Int J Heat Mass Transfer* 1993;36:674–683.
13. Rabin Y, Shitzer A. Numerical solution of the multidimensional freezing problem during cryosurgery. *J Biomech Eng* 1998;120:32–37.
14. Rewcastle JC, Sandison GA, Hahn LJ, Saliken JC, McKinnon JG, Donnelly BJ. A model for the time-dependent thermal distribution within an iceball surrounding a cryoprobe. *Phys Med* 1998;43:3519–3534.
15. Richmond MA, Murphy CA, Pouzet B, Schmid P, Rawlins JN, Feldon J. A computer controlled analysis of freezing behaviour. *J Neurosci Methods* 1998;86: 91–99.
16. Tatsutani K, Rubinski B, Onik G, Dahiya R. Effect of thermal variables on frozen human primary prostatic adenocarcinoma cells. *Urology* 1996;48:441–447.
17. Tong DD, Fenster A. Three dimensional ultrasound prostate imaging system. *Ultrasound Med Biol* 1996; 22:735–745.
18. Von Eschenbach A, Ho R, Murphy GP, Cunningham M, Lins N. American Cancer Society guidelines for the early detection of prostate cancer: Update 1997. *Ca Cancer J Clin* 1997;47:261–264.
19. Wong WS, Chinn DO, Chinn M, Chinn J, Tom WL. Cryosurgery as a treatment of prostate carcinoma. *Cancer* 1997;79:963–974.